The Use of Extensional Rheometry to Establish Operating Parameters for Stretching Processes

GLEN H. PEARSON and RICHARD W. CONNELLY, *Research Laboratories, Eastman Kodak Company, Rochester, New York 14650*

Synopsis

This work describes a method of determining the limits of uniform extensibility, in terms of failure and fracture, from rheological tests in extensional flow. The limit of uniform stretching can be expressed in terms of the Weissenberg number for the process, as demonstrated by data for three chemically diverse polymers, polystyrene, poly(methyl methacrylate), and a polyester. The BKZ–K model can be used to predict necking failure, as determined by the Considère criterion, and an empirical correlation can be derived for fracture.

INTRODUCTION

Over the past decade there have been numerous investigations of the response of polymers, both in the melt and in solution, to extensional flow. The objective of much of the work has been to measure the extensional viscosity η_e as a function of strain rate. Notable among the recent efforts are the papers of Munstedt[1,2] and Meissner,[3,4] who used polyethylene, a material with a low flow activation energy.

Although some attempts have been made to correlate the results of extensional rheometry with processing performance, a clear, unifying picture of the behavior of polymer melts to extensional flows encountered in processing does not exist. A series of papers by White and Ide[5–8] described fracture in extensional flow, relevant to melt spinning, using a convected Maxwell model with a deformation-rate-dependent viscosity and relaxation time. Owing to the model's simplicity, the comparison with data for low-density polyethylene, polystyrene, high-density polyethylene, and poly(methyl methacrylate) was qualitative. More recently, Lobe and Macosko[9] used a Bogue–White model[10] to predict the performance of polymeric toners in an electrophotographic copying process, and Connelly and Pearson[11] used a BKZ model[12] to predict cohesive strength in an adhesive subjected to a 180°C peel test.

Although considerable success has been achieved with single-integral models in predicting extensional response, statements concerning the unpredictability of response and differences in response from material to material still persist. In this work, polymers of different chemical structure were chosen to investigate the limits of uniform stretching and fracture and to provide a unifying framework for process design. The materials used, a polystyrene (PS), a poly(methyl methacrylate) (PMMA), and a polyester (POCH), are listed in Table I with information concerning molecular weight, molecular-weight distribution, and the glass-transition temperature. All of the polymers have broad molecular-weight distributions and are typical of commercial polymers.

Journal of Applied Polymer Science, Vol. 27, 969–981 (1982)
 CCC 0021-8995/82/030969-13$01.30

TABLE I
Molecular and Rheological Properties

Polymer	$P_W^a \times 10^{-4}$	P_W/P_N	T_g (°C)[b]	T_{ref} (°C)	$\eta_0(p) \times 10^{-6}$	a_b	τ_M (s)
PMMA	7.53	2.03	110	180	5.0	0.28	9.8
POCH[c]	4.91	1.87	43	86	2.5	0.3	2.1
PS	27.1	5.3	105	210	0.11	0.24	0.99

[a] Polystyrene-equivalent molecular weight by gel permeation chromatography.
[b] 10°C/min heating rate, differential scanning calorimetry.
[c] Copolyester of terephthalic acid and 50:50 diethylene glycol and neopentyl glycol.

MATERIAL CHARACTERIZATION

A common series of tests performed to characterize a given polymer melt's rheological behavior might include:

1. Small-amplitude sinusoidal shearing to determine the linear viscoelastic moduli, G' (storage) and G'' (loss), as a function of frequency (ω) and to measure the temperature sensitivity of the rheological response through the use of time–temperature superposition to determine the shift factors (a_T).
2. Low-shear-rate rheometry, typically $\dot{\gamma} < 1\ s^{-1}$, using a cone-and-plate geometry to determine the zero-shear-rate viscosity(η_0),

$$\eta_0 = \lim_{\dot{\gamma} \to 0} \eta(\dot{\gamma}) \tag{1}$$

the viscosity (η), and first normal stress difference ($N_1 = \sigma_{11} - \sigma_{22}$).
3. High-shear-rate viscometry to measure the dependence of viscosity upon shear rate.

Generally, after such a battery of tests is performed, the characterization for practical purposes, that is, to determine why polymer A worked in a given process while polymer B did not, is complete. Extensional tests are contemplated only when the experiments listed above fail to show a difference. The premise of this paper is that, in many cases, proper characterization, as outlined above, coupled with the predictions of a viscoelastic constitutive model is sufficient to characterize the extensional response of a polymer melt in a typical process flow such as blow molding or film stretching.

To demonstrate the validity of this premise, we used the procedure outlined above to fully characterize the materials to be studied: PS, PMMA, and POCH. As will be shown, this is the minimum characterization required to specify the constitutive model for any specific material. After the normal rheological characterization was complete, the extensional response was obtained by using the fixtures shown in Figure 1, which are mounted in a Rheometrics mechanical spectrometer (RMS) capable of performing orthogonal rheometry. In the experiment, rods of the melt to be tested are formed by slow extrusion through a capillary tube. A small bead of epoxy is placed on one end of the rod and cured overnight. The rod is placed in the RMS by threading it through a spindle placed on the stationary post (left post in Figure 1) and initially wound about the right fixture, which will rotate. After a period of time to ensure uniform temperature, the right winder is caused to rotate and the rod is subsequently extended. The operator must raise the rotating rod to prevent the polymer from winding upon itself, as the strain rate is determined by the winder diameter D from

$$\dot{\epsilon}(t) = \Omega(t)D/2L \tag{2}$$

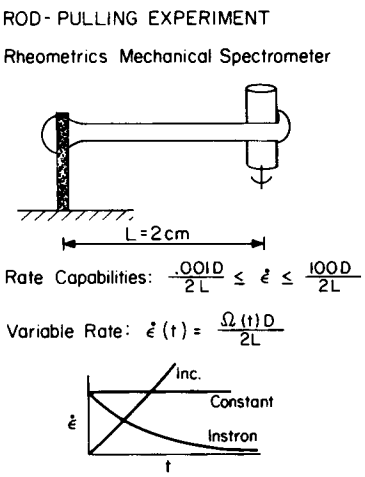

Fig. 1. Sketch of stretching apparatus used with the Rheometrics mechanical spectrometer.

where $\Omega(t)$ is the rotational speed, L is the length between fixtures, and $\dot{\epsilon}$ is the strain rate. Since the rotational speed can be programmed by controlling the RMS motor, it is possible to achieve any strain-rate program desired. The stress is calculated from the force measured on the stationary fixture divided by a calculated change in cross-sectional area:

$$\sigma_{11} - \sigma_{22} = F(t)/A(t) \tag{3}$$

If one assumes an incompressible melt and uniform uniaxial extension, then the cross-sectional area is related to the strain rate by

$$A(t) = A(0) \exp[-\int_0^t \dot{\epsilon}(t')dt'] \tag{4}$$

Previous work showed that materials with high elasticity could be stretched uniformly to high extensions in this type of experiment.[13]

A final note on characterization concerns the use of a viscoelastic constitutive model to predict material response. A BKZ constitutive equation was chosen with a memory function suggested by Kaye and Kennett.[14] The model expresses the stress as a single integral of strain over all past time

$$\sigma = \int_{-\infty}^{t} N(t - t', I_c)\mathbf{C}^{-1}(t, t')dt' \tag{5a}$$

with a strain-history-dependent memory function

$$N(t - t', I_c) = \sum_{n=1}^{N} \frac{G_n}{\tau_n} \exp\left[\frac{-(t - t')}{\tau_n}\right] \exp(-a_b\sqrt{I_c - 3}) \tag{5b}$$

This model is very similar to that recently proposed by Wagner.[15,16]

To determine the material constants G_n, τ_n, and a_b for the BKZ–K model, we adopted the following scheme:

1. From the linear viscoelastic moduli, G' and G'', $H(\tau)$, the relaxation function as a function of τ, was calculated by using the Ninomiya–Ferry technique.[17]

2. The set of moduli, G_n, and relaxation times τ_n were determined from $H(\tau)$ vs. $\ln \tau$ by integrating

$$\eta_0 = \int_{-\infty}^{\infty} H(\tau) \cdot \tau d \ln \tau \tag{6}$$

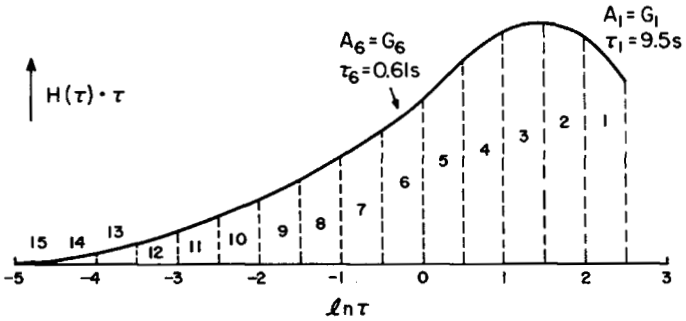

Fig. 2. Sketch illustrating the method of obtaining $[G_n, \tau_n]$ from the relaxation function $H(\tau)$.

in a piecewise fashion and assuming that the integrand of each step is G_n while τ_n is the midpoint of the step, as illustrated by Figure 2. This procedure is due to Bogue.[18]

3. After checking the fit of the relaxation spectrum to the linear viscoelastic moduli from which it was calculated using

$$G' = \sum_{n=1}^{N} \frac{G_n \tau_n^2 \omega^2}{1 + (\tau_n \omega)^2} \tag{7}$$

$$G'' = \sum_{n=1}^{N} \frac{G_n \tau_n \omega}{1 + (\tau_n \omega)^2} \tag{8}$$

derived from Eqs. (5a) and (5b), the prediction of $\eta(\dot{\gamma})$ was obtained for the case $a_b = 1$.

$$\eta(\dot{\gamma}) = \sum_{n=1}^{N} \frac{G_n \tau_n}{(1 + a_b \tau_n \dot{\gamma})^2} \tag{9}$$

A horizontal shift of the line predicted by Eq. (9) with $a_b = 1$ to obtain coincidence with data for $\eta(\dot{\gamma})$ then yields the value of a_b, generally 0.2–0.3, for the melt being studied.

4. To check the validity of the fit for shearing deformations, N_1 may be predicted using

$$N_1 = \sum_{n=1}^{N} \frac{G_n \tau_n^2 \dot{\gamma}^2}{(1 + a_b \tau_n \dot{\gamma})^3} \tag{10}$$

An analytical, closed-form expression to predict extensional viscosity η_e or the extensional stress growth during extension is not possible with this model. Predictions are obtained, once the model parameters are determined, from a solution of the integral form

$$\sigma_{11} - \sigma_{22} = \int_{-\infty}^{t} N(t - t', I_c)[C_{11}^{-1}(t', t) - C_{22}^{-1}(t', t)]dt' \tag{11}$$

where the components of the Finger tensor are given by

$$\mathbf{C}^{-1}(t', t) = \begin{pmatrix} \left[\frac{L(t)}{L(t')}\right]^2 & 0 & 0 \\ 0 & \left[\frac{L(t)}{L(t')}\right]^{-1} & 0 \\ 0 & 0 & \left[\frac{L(t)}{L(t')}\right]^{-1} \end{pmatrix} \tag{12}$$

for $t' > 0$ and

$$\mathbf{C}^{-1}(t', t) = \begin{pmatrix} \left[\frac{L(t)}{L(0)}\right]^2 & 0 & 0 \\ 0 & \left[\frac{L(t)}{L(0)}\right]^{-1} & 0 \\ 0 & 0 & \left[\frac{L(t)}{L(0)}\right]^{-1} \end{pmatrix} \tag{13}$$

for $t' \leq 0$, and the first variant of the strain tensor, I_c, is

$$I_c = \left[\frac{L(t)}{L(t')}\right]^2 + 2\left[\frac{L(t)}{L(t')}\right]^{-1} \tag{14}$$

for $t' > 0$ and

$$I_c = \left[\frac{L(t)}{L(0)}\right]^2 + 2\left[\frac{L(t)}{L(0)}\right]^{-1} \tag{15}$$

for $t' \leq 0$.

RESULTS AND DISCUSSION

The results of the linear viscoelastic and steady-shearing tests are shown in Figures 3 and 4, which give the linear viscoelastic moduli G'' and G' as a function of frequency. Figure 5 shows the steady-shear viscosity and first normal stress difference. For each material, an arbitrary reference temperature was chosen.

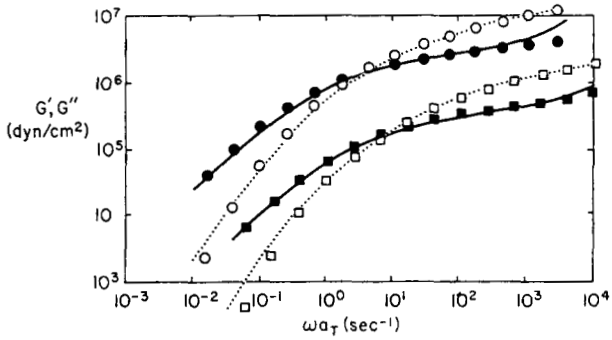

Fig. 3. Linear viscoelastic moduli vs. frequency for PS (□, ■) and POCH (○, ●) compared with the BKZ–K prediction. The predictions are represented by the lines: G'' (—) and G' (- - -).

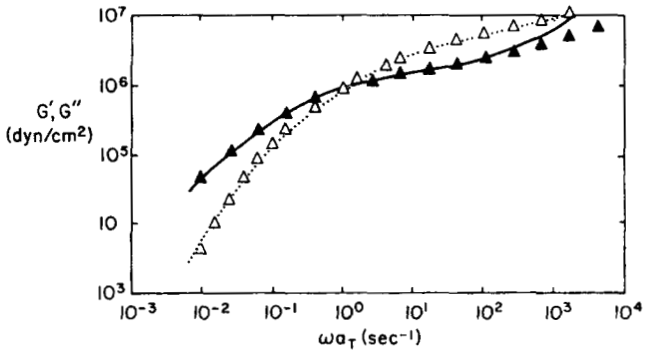

Fig. 4. Linear viscoelastic moduli vs. frequency for PMMA (△, ▲) compared with the BKZ–K prediction. The predictions are represented by lines: G'' (—) and G' (- - -).

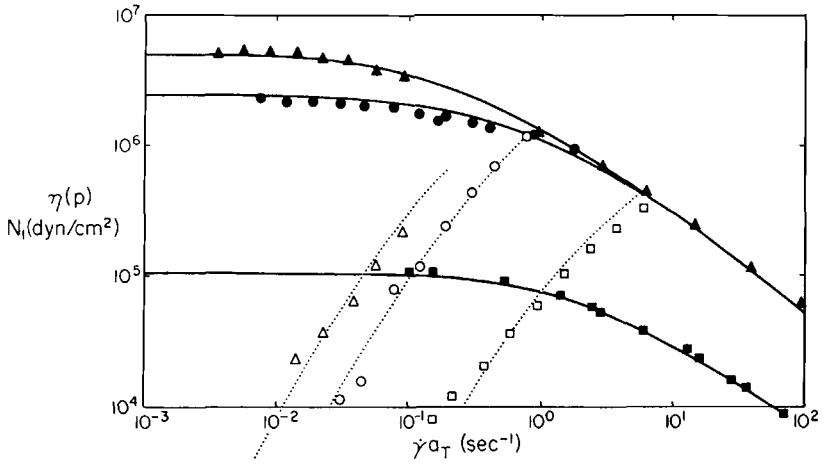

Fig. 5. Shear viscosity (open symbols) and first normal stress difference (filled symbols) vs. shear rate for each sample compared with the BKZ–K prediction. (▲, △) PMMA; (●, ○) POCH; (■, □) PS.

The lines in each figure represent the fit of the BKZ–K model, which was quite satisfactory in all cases. Values of a_b and τ_M, which is defined as

$$\tau_M = \sum_{n=1}^{N} G_n \tau_n^2 \Big/ \sum_{n=1}^{N} G_n \tau_n \tag{16}$$

are given in Table I for each sample. τ_M is the weight-average maximum relaxation time used by Graessley.[19]

The extensional flow response is shown in Figures 6–8. In each figure, true stress–time data are shown for constant rates of extension as well as an "Instron" strain-rate program, for which

$$\dot{\epsilon} = \frac{\dot{\epsilon}_0}{1 + \dot{\epsilon}_0 t} \tag{17}$$

Again, the lines represent the fit of the BKZ–K model and demonstrate the

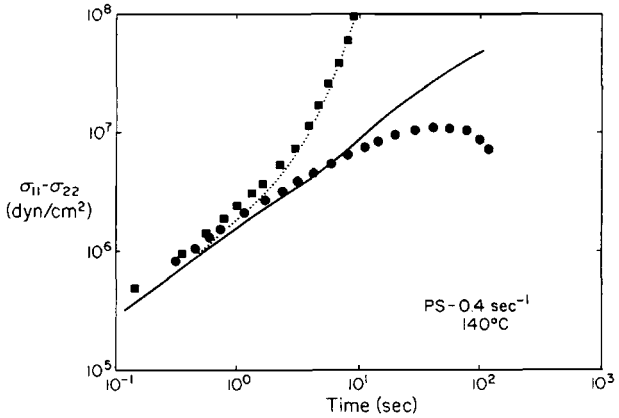

Fig. 6. Extensional-flow data for constant (■) and "Instron-type" (●) extensions compared with the BKZ–K predictions for PS.

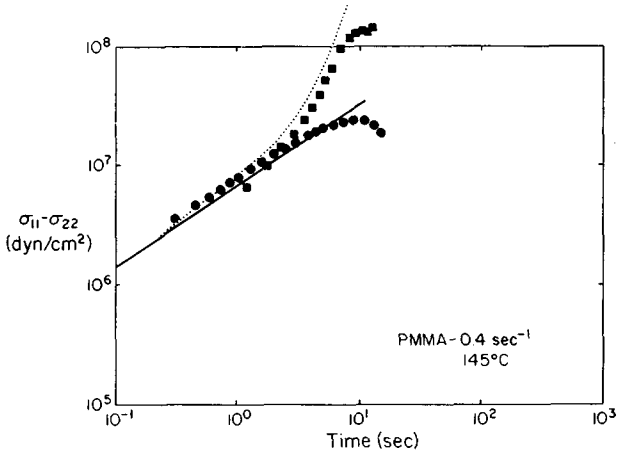

Fig. 7. Extensional-flow data for constant (■) and "Instron-type" (●) extensions compared with the BKZ–K predictions for PMMA.

predictive capability of the model. At short times or small strains, the model fits the data quite well in all cases. At longer times some deviation is apparent. For both PS and PMMA the model overpredicts the observed stress.

Despite our ability to measure the flow response of melts in extensional flow and to predict this reponse with the BKZ–K model, we still have the question as to the utility of either the data or the model to predict material response to processing flows. As mentioned earlier, stretch uniformity and fracture are two major concerns in extensional-flow-dominated processes such as blow molding, film fabrication, and stretch coating. An operational criterion for fracture is readily apparent, but uniformity poses a problem. Vincent,[20] in a paper based on earlier work on metals by Orowan,[21] stated that the Considére criterion asserts that uniformity of stretching is guaranteed if the process operates such that the strain is less than ϵ_F, which is the strain at which a maximum occurs in the force–extension curve. This strain corresponds to the yield point in a stress–elongation curve, as shown in Figure 9. If the process operates at higher strains, then uniformity is not necessarily obtained, and if, for instance, temperature

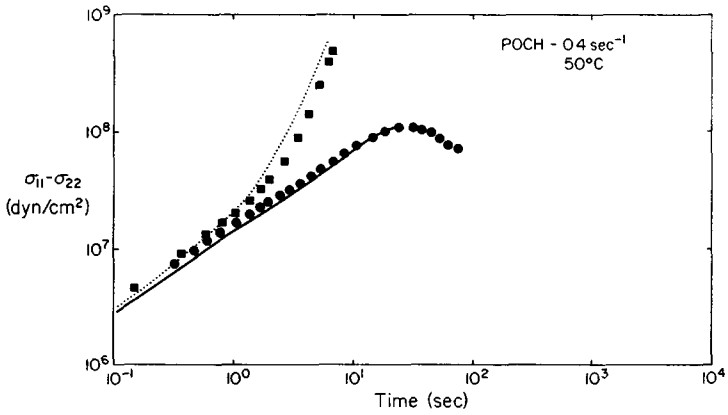

Fig. 8. Extensional-flow data for constant (■) and "Instron-type" (●) extensions compared with the BKZ–K predictions for POCH.

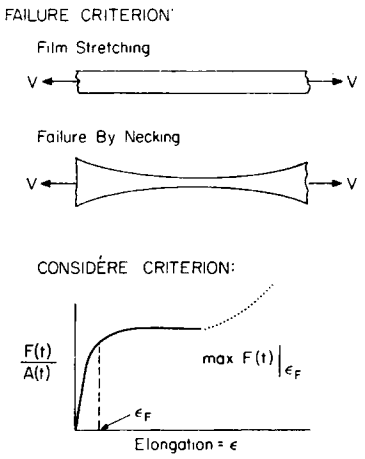

Fig. 9. Sketch of force-extension curve showing point of incipient failure.

nonuniformities existed, inducing different force responses in a stretch process at two given points, both points could be in "equilibrium" relative to Figure 9 and thus lead to a nonuniform stretching operation. The strain at the maximum force ϵ_F will be used as the operational criterion for failure of uniform extension.

Figures 10 and 11 give representative data of ϵ_F vs. $\dot{\epsilon}$ for PMMA and ϵ_F vs. $\dot{\epsilon}_0$ for POCH. Also shown are the BKZ–K predictions, which are in good agreement with the data, particularly with the magnitude and trend of ϵ_F with strain rate. Once the data for each sample are compiled, they are reduced to a single plot of ϵ_F vs $\tau_M\dot{\epsilon}$, the Weissenberg number (Fig. 12). The data in Figure 12 are independent of temperature, as both $\dot{\epsilon}$ and τ_M shift with the same factor, a_T. The correlation of the data with the single factor τ_M is extremely important in light of the sensitivity of the model predictions for η_e to slight variations of a_b, which do exist (see Table I). The extensional viscosity vs. $\dot{\epsilon}a_T$ predicted by the BKZ–K model is shown in Figure 13 for the materials used. The predicted extensional viscosity normalized response shows that PS, which has the smallest value of

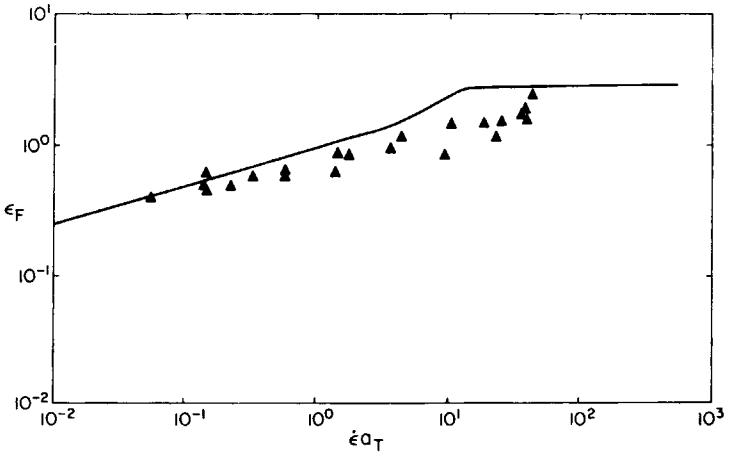

Fig. 10. ϵ_F vs. $\dot{\epsilon}a_T$ for PMMA, T_{ref} = 180°C. The line is the BKZ–K prediction.

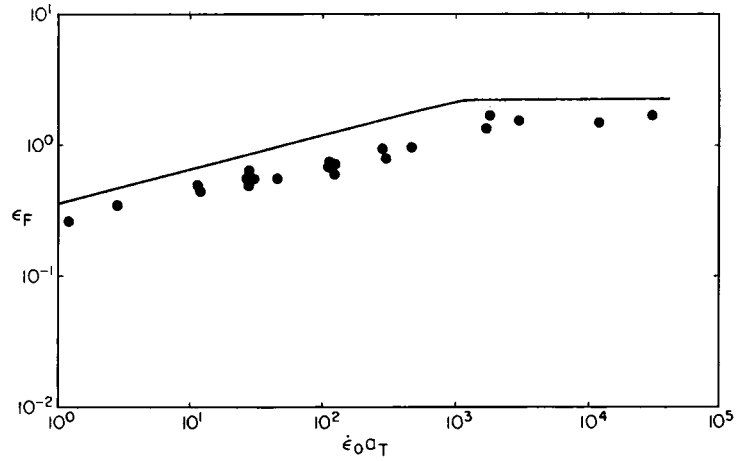

Fig. 11. ϵ_F vs. $\dot{\epsilon}_0 a_T$ for POCH, $T_{ref} = 86°C$. The line is the BKZ–K prediction.

a_b, has the highest maximum η_e/η_0. Although there are differences in the predicted extensional viscosity, which is a steady-state property of the material, these differences are not apparent in the transient data presented here. Neither are they apparent in the prediction of the BKZ–K model for ϵ_F vs. $\tau_M\dot{\epsilon}$, which is shown as the single line in Figure 12.

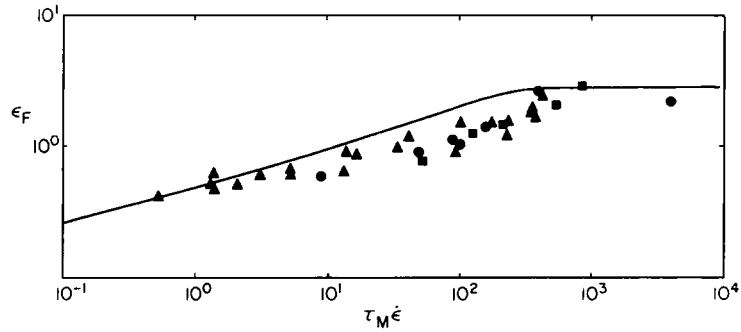

Fig. 12. Master curve of ϵ_F vs. $\tau_M\dot{\epsilon}$ for all samples. (▲) PMMA; (●) POCH; (■) PS.

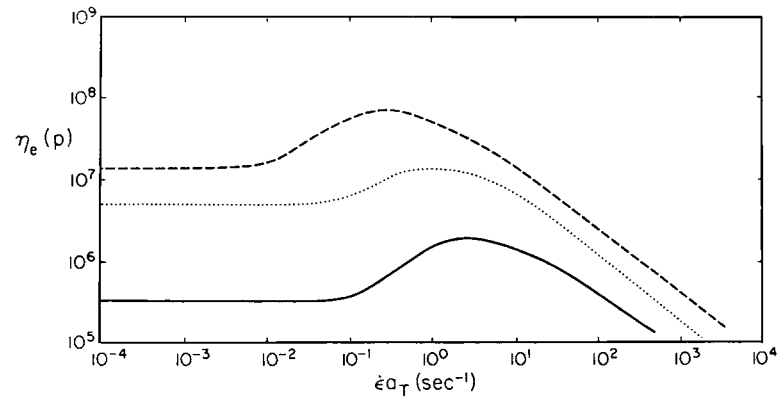

Fig. 13. Predicted extensional viscosity vs. $\dot{\epsilon}a_T$ for all samples. (- - -) PMMA; (. . .) POCH; (—) PS.

The results for the "Instron-type" rate program are shown in Figure 14, plotted as ϵ_F vs. $\tau_M\dot{\epsilon}_0$. Again, the data show good correlation for the various polymer samples. Interestingly, the Hencky strain-to-fail for a decreasing-rate extension is very similar to a constant-rate extension until high extension rates are reached. (These rates are relative to a reference temperature. The actual limit of the experiment is roughly 4 s^{-1}.) At these high rates, ϵ_F seems to plateau at a value of 2 for an Instron-rate program and 3 for a constant-rate extension. The BKZ model predicts plateau values of ϵ_F of 2.2 and 2.8 for Instron- and constant-rate extensions, respectively.

For fracture, although a simple observation suffices to note its occurrence, no straightforward method is available to predict it. Based on the experiments performed as part of this work, some empirical means of correlating data seems plausible. Several correlations were attempted. Figure 15 shows the tensile-stress-at-break vs. the time-to-break normalized to a reference temperature and by the maximum relaxation time. Considerable scatter exists in the data, as is expected from this type of experiment; however, a reasonable correlation exists. Figure 16 demonstrates the use of the work-to-break W_B, defined as

$$W_B = \int_0^{\lambda_B - 1} (F/A_0)d(\lambda - 1) \tag{18}$$

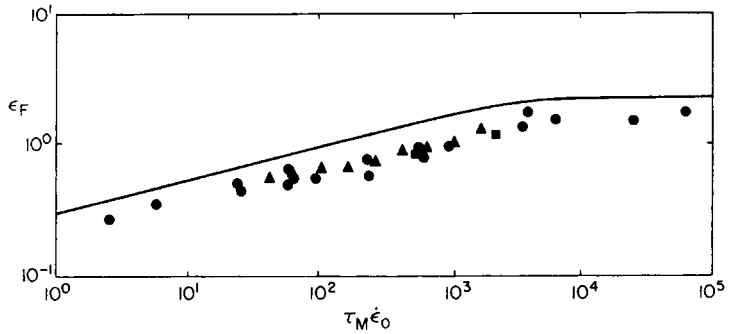

Fig. 14. ϵ_F vs. $\tau_M\dot{\epsilon}_0$ for all samples. The line is the BKZ–K prediction. (▲) PMMA; (●) POCH; (■) PS.

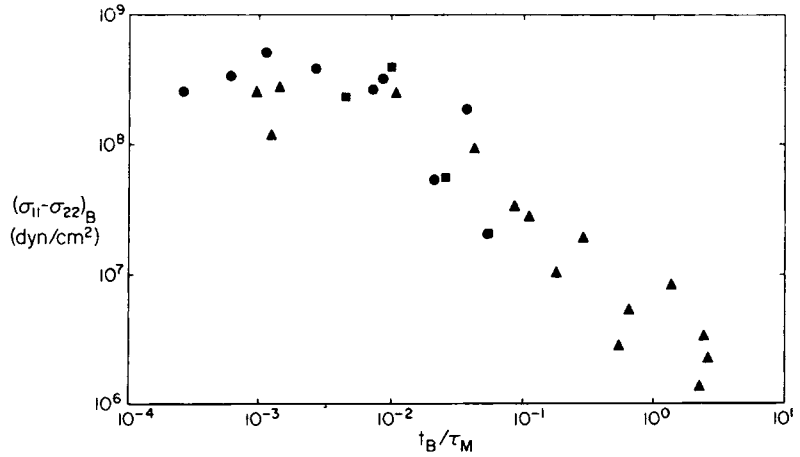

Fig. 15. Tensile-stress-at-break vs. time-to-break normalized by τ_M for all samples. (▲) PMMA; (●) POCH; (■) PS.

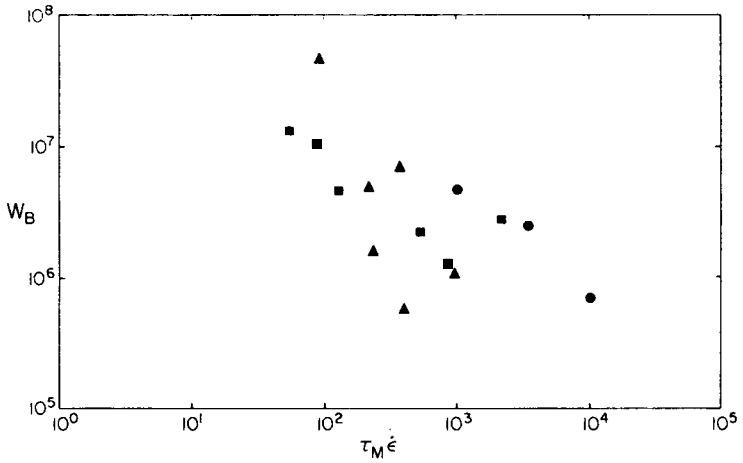

Fig. 16. W_B vs. $\tau_M \dot{\epsilon}$ for all samples from eq. (4). (▲) PMMA; (●) POCH; (■) PS.

vs. $\tau_M \dot{\epsilon}$ to predict fracture. The correlation looks about as good as the stress-to-break vs. time-to-break method. When the Hencky strain-to-break is plotted vs. $\dot{\epsilon}\tau_M$, as in Figure 17, a reasonable correlation exists for all the materials when the degree of scatter is considered. Furthermore, experiments on POCH with the Instron-rate program allowed a fit of ϵ_B vs. $\tau_M \dot{\epsilon}_0$ using the expression

$$\epsilon_B = 3.35 + \ln[(1 + 1.48\,(10^{-3})\tau_M \dot{\epsilon}_0)^2]^{-0.125} \tag{19}$$

This line is drawn on Figure 17 for comparison and fits the data for constant rate surprisingly well. The results of the experiments concerning fracture indicate that this last correlation of ϵ_B vs. $\tau_M \dot{\epsilon}$ may be useful as a first approximation for fracture in these polymers which are chemically diverse. Considering the amount of scatter in Figures 15–17, more work is necessary before a satisfactory correlation is available. The recent work of Vinogradov and his co-workers[22] and that of Crissman and Zapas[23,24] may prove useful. Meissner et al.[4] have shown that Hencky strains of 7 can be obtained without fracture using low-density polyethylene at low rates and high temperatures. This information may indicate an upturn in the correlation of Figure 17 at low strain rates.

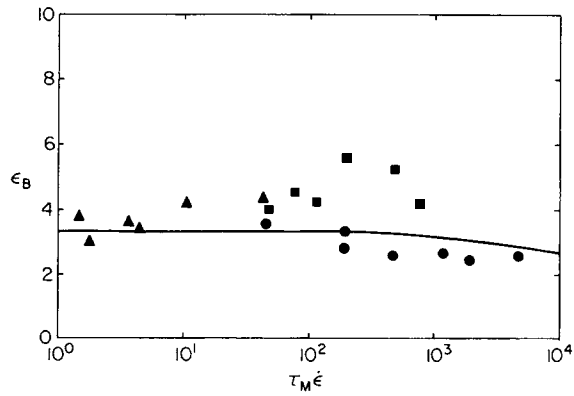

Fig. 17. ϵ_B vs. $\tau_M \dot{\epsilon}$ for all samples. (▲) PMMA; (●) POCH; (■) PS.

SUMMARY

Extensional flow in polymer processing steps is quite commonly a low-temperature, nonisothermal, high-nonconstant-rate deformation. In the design of these processes, two of the major concerns are uniformity of and fracture during stretching. This work with three chemically diverse polymers, poly(methyl methacrylate), polystyrene, and a polyester, has shown that the limit of uniform stretching as established by the strain to reach a maximum in the force–elongation curve limit is a function of the Weissenberg number $\tau_M\dot{\epsilon}$. Reasonable predictions of ϵ_F vs. $\tau_M\dot{\epsilon}$ can be made using the BKZ–K model. Fracture of the material also can be correlated and predicted, to a first approximation, by the Weissenberg number, although considerable scatter exists in the data. Interestingly, data for the constant-strain-rate and the Instron-rate programs are indistinguishable.

NOMENCLATURE

A_0	initial cross-sectional area of sample
a_b	parameter in BKZ–K memory function
a_T	time-temperature superposition factor
$\mathbf{C}^{-1}$	Finger strain tensor
F	force during extension
G'	storage modulus
G''	loss modulus
G_n	discrete modulus in relaxation spectrum
$H(\tau)$	relaxation function
I_c	first invariant of Finger strain tensor
$N(t-t', I_c)$	memory function for BKZ–K model
t	time
W_B	work to break

Greek

$\dot{\epsilon}$	strain rate
$\dot{\epsilon}_0$	initial strain rate in "Instron-type" extension
ϵ_F	strain to fail
ϵ_B	strain to break
$\dot{\gamma}$	shear rate
λ	engineering strain
λ_B	engineering strain to break
η	shear viscosity
η_e	extensional viscosity
Ω	rotational velocity
ω	frequency
σ	deviatoric stress tensor
τ_M	maximum relaxation time
τ_n	nth relaxation time in discrete relaxation spectrum

We acknowledge the work of Mr. J. Wesson in obtaining molecular-weight information and Dr. L. J. Garfield for many stimulating discussions during the early stages of this work.

References

1. H. M. Laun and H. Munstedt, *Rheol. Acta*, **17**, 415 (1978).
2. H. Munstedt, *Rheol. Acta*, **14**, 1077 (1975).
3. J. Meissner, *Trans. Soc. Rheol.*, **16**, 405 (1972).
4. T. Raible, A. Demarmels, and J. Meissner, *Polym. Bull.*, **1**, 397 (1979).
5. Y. Ide and J. L. White, *J. Appl. Polym. Sci.*, **20**, 2511 (1976).
6. Y. Ide and J. L. White, *J. Non-Newt. Fluid Mech.*, **2**, 281 (1977).
7. Y. Ide and J. L. White, *J. Appl. Polym. Sci.*, **22**, 1061 (1978).
8. J. L. White and Y. Ide, *J. Appl. Polym. Sci.*, **22**, 3057 (1978).
9. V. M. Lobe and C. W. Macosko, Society of Rheology Meeting, Boston, Mass., October 1979.
10. D. C. Bogue and I. J. Chen, *Trans. Soc. Rheol.*, **16**, 59 (1972).
11. R. W. Connelly and G. H. Pearson, Society of Rheology Meeting, Boston, Mass., October 1979.
12. B. Berstein, E. Kearsley, and L. Zapas, *Trans. Soc. Rheol.*, **7**, 391 (1963).
13. R. W. Connelly, L. J. Garfield, and G. H. Pearson, *J. Rheol.*, **23**, 651 (1979).
14. A. Kaye and A. J. Kennett, *Rheol. Acta*, **13**, 916 (1974).
15. M. H. Wagner, *Rheol. Acta*, **15**, 133 (1976).
16. M. H. Wagner, *Rheol. Acta*, **15**, 136 (1976).
17. K. Ninomiya and J. D. Ferry, *J. Colloid Sci.*, **14**, 36 (1959).
18. D. C. Bogue, *IEC Fund.*, **5**, 253 (1966).
19. W. W. Graessley, *Adv. Polym. Sci.*, **16**, 1 (1974).
20. P. I. Vincent, *Polymer*, **1**, 7 (1960).
21. F. Orowan, *Rep. Prog. Phys.*, **12**, 186 (1949).
22. E. K. Bovisenkova, O. Yu. Sabsai, M. K. Kurbanaliev, V. E. Dreval, and G. V. Vinogradov, *Polymer*, **19**, 1473 (1978).
23. J. M. Crissman and L. J. Zapas, *Polym. Eng. Sci.*, **19**, 99 (1979).
24. L. J. Zapas and J. M. Crissman, *Polym. Eng. Sci.*, **19**, 104 (1979).

Received January 27, 1981
Accepted September 14, 1981